ASN NEURO RESEARCH ARTICLE

Supplementary data

ASN NEURO 2(3):art:e00035.doi:10.1042/AN20090059

Glial glucokinase expression in adult and post-natal development of the hypothalamic region

Carola Millán*[2], Fernando Martínez*[2], Christian Cortés-Campos*, Isabel Lizama*, Maria Jose Yañez*, Paula Llanos*, Karin Reinicke[†], Federico Rodríguez[†], Bruno Peruzzo[‡], Francisco Nualart[†1] and Maria Angeles García*[1]

*Laboratorio de Biología Celular, Departamento de Biología Celular, Facultad de Ciencias Biológicas, Universidad de Concepción, Concepción, Chile
[†]Laboratorio de Neurobiología, Departamento de Biología Celular, Facultad de Ciencias Biológicas, Universidad de Concepción, Concepción, Chile
[‡]Instituto de Anatomía, Histología y Patología, Universidad Austral de Chile, Valdivia, Chile

Cite this article as: Millán C, Martínez F, Cortés-Campos C, Lizama I, Yañez MJ, Llanos P, Reinicke K, Rodríguez F, Peruzzo B, Nualart F and García MA (2010) Glial glucokinase expression in adult and post-natal development of the hypothalamic region. ASN NEURO 2(3):art:e00035.doi:10.1042/AN20090059

ABSTRACT

It has recently been proposed that hypothalamic glial cells sense glucose levels and release lactate as a signal to activate adjacent neurons. GK (glucokinase), the hexokinase involved in glucose sensing in pancreatic β-cells, is also expressed in the hypothalamus. However, it has not been clearly determined if glial and/or neuronal cells express this protein. Interestingly, tanycytes, the glia that cover the ventricular walls of the hypothalamus, are in contact with CSF (cerebrospinal fluid), the capillaries of the arcuate nucleus and adjacent neurons; this would be expected for a system that can detect and communicate changes in glucose concentration. Here, we demonstrated by Western-blot analysis, QRT–PCR [quantitative RT–PCR (reverse transcription–PCR)] and *in situ* hybridization that GK is expressed in tanycytes. Confocal microscopy and immunoultrastructural analysis revealed that GK is localized in the nucleus and cytoplasm of β1-tanycytes. Furthermore, GK expression increased in these cells during the second week of post-natal development. Based on this evidence, we propose that tanycytes mediate, at least in part, the mechanism by which the hypothalamus detects changes in glucose concentrations.

Key words: arcuate nucleus, brain, glia, glucokinase, glucosensing, tanycyte.

INTRODUCTION

The hypothalamus has been associated with the modulation of feeding behaviour and corporal growth due to its ability to detect changes in blood glucose. It has been proposed that metabolic interactions between glial cells and neurons may be required for glucose sensing in the brain a short time after feeding. Thus the glycolytic metabolism of glucose by glial cells and transfer of lactate to neighbouring neurons may lead to enhanced ATP synthesis in the latter and thus contribute to the closure of K_{ATP} channels (Ainscow et al., 2002).

Hypothalamic neurons are associated with highly elongated glial cells, namely tanycytes. There are four different types of tanycytes, α1, α2, β1 and β2 (Akmayev and Popov, 1977). The α2- and β1-tanycytes are localized in the lower lateral wall of the third ventricle and develop cell processes that contact neurons in the arcuate nucleus as well as capillaries in the hypothalamus (Garcia et al., 2001). Thus periventricular hypothalamic tanycytes, which contact the CSF (cerebrospinal fluid) and the neuronal soma, may metabolically couple neurons from the arcuate and the ventromedial nucleus, regulating glucose-sensing activities. We demonstrated that GLUT2 (glucose transporter 2) is expressed in tanycytes; however, we observed a reduced hybridization and immunohistochemical reactivity of GLUT2 in neuronal soma, indicating low-to-absent expression of GLUT2 in arcuate nucleus neurons (Garcia et al., 2003). The expression of GLUT2 in α- and β-tanycytes suggests that tanycytes contacting ventromedial hypothalamic neurons (α) and arcuate nucleus neurons (β) are involved in glucose uptake using the same low-affinity transporter. In both types of cells, the localization of GLUT2 is observed in the proximal pole of tanycytes, which contacts the CSF (Garcia et al., 2003). Thus tanycytes may be primarily involved in detecting glucose concentration in the CSF of the ventricular system. Similar localization of GLUT2 and GK (glucokinase) has been detected in ependymal cells of the cerebral aqueduct and dorsal third ventricle (Maekawa et al., 2000), indicating that

[1] Correspondence may be addressed to either of these authors (email frnualart@udec.cl or mgarcia@udec.cl).
[2] These authors contributed equally to the present study.
Abbreviations: CSF, cerebrospinal fluid; DIG, digoxigenin; DTT, dithiothreitol; GFAP, glial fibrillary acidic protein; GLUT2, glucose transporter 2; GK, glucokinase; GKRP, GK regulatory protein; RT–PCR, reverse transcription–PCR; TFIIB, transcription factor IIB.

different cells facing the ventricular system may be involved in glucose sensing.

GK plays a fundamental role in glucose homoeostasis, catalysing the high-K_m phosphorylation of glucose in different tissues involved in glucose sensing. Glucose is transported by GLUT2, which has a high K_m for glucose, and then glucose is phosphorylated by GK or hexokinase IV. GK has a low affinity for phosphorylating glucose (K_m=10–15 mM), and the enzyme is not inhibited by glucose-6-phosphate. Mice lacking β-cell GK die within 3 days of birth from acute hyperglycaemia (Bali et al., 1995; Terauchi et al., 1995). Hepatic GK is regulated at a post-translational level through binding to GKRP (GK regulatory protein), which functions as an anchor protein, modulating GK activity and mediating its nuclear translocation (Vandercammen and Van Schaftingen, 1990, 1991). In normoglycaemia, GK is detected in both the nuclei and cytoplasm of parenchymal cells (Toyoda et al., 1995a). GK mRNA was selectively identified by RT (reverse transcription)–PCR as well as *in situ* hybridization in rat hypothalamus (Kang et al., 2004, 2006; Yang et al., 1999). At the protein level, immunoblotting and enzyme assays have confirmed the presence of GK in rat and human hypothalamic extracts (Roncero et al., 2000, 2004). GK is expressed in the hypothalamus, regulating reproductive function, glucocorticoid secretion, food intake and hypothalamic gene expression (Yang et al., 2007). Thus GK plays a key role in the neuroendocrine regulation of metabolic economy. Kang et al. (2006) confirmed that GK is a critical regulator of neuronal activity in freshly dissociated ventromedial hypothalamic nucleus neurons.

The hypothesis that the hypothalamus can detect changes in glucose levels requires the identification of the cells involved in this process. Consequently, the aim of the present study was to study whether tanycytes express GK and to define its subcellular distribution in the hypothalamic periventricular region.

MATERIALS AND METHODS

Animals

We used adult Sprague–Dawley rats. The Animal Experimentation Committee at the University of Concepcion, Faculty of Biological Science, approved all animal experiments.

Immunocytochemistry

Rat brain samples (Sprague–Dawley) were dissected and fixed directly by immersion in 4% (w/v) paraformaldehyde (12 h) or cold (−20°C) methanol (2 h). Thick transverse sections (40 μm) were cut with a cryostat, and the sections were processed free-floating. For immunohistochemical co-localization analyses, we used the following antibodies and dilutions: anti-GLUT2 (1:100, Alpha Diagnostic International, San Antonio, TX, U.S.A.), rabbit anti-GFAP (glial fibrillary acidic protein; Dako, Campintene, CA, U.S.A.), mouse anti-vimentin (1:100; Boehringer–Mannheim, Mannheim, Germany), rabbit anti-GK (1:50, sc7908; Santa Cruz Biotechnology, Santa Cruz, CA, U.S.A.), and sheep anti-GK (1:200, provided by Dr Mark Magnuson, Vanderbilt University, Nashville, TN, U.S.A.). Sections were incubated with the antibodies overnight at 20°C in a humid chamber. The antibodies were diluted in a Tris/HCl buffer (pH 7.8) containing 8.4 mM sodium phosphate, 3.5 mM potassium phosphate, 120 mM NaCl and 1% BSA. After extensive washing, the liver or pancreas sections were incubated for 2 h at 20°C with peroxidase-labelled anti-rabbit IgG (1:100; Dako). The peroxidase activity was developed using a DAB (diaminobenzidine) substrate kit (ImmunoPure; Pierce Biotechnology, Rockford, IL, U.S.A.). For immunofluorescence and co-localization analyses, the brain tissues were incubated with the primary antibodies overnight and additionally with Cy2- or Cy3-labelled secondary antibodies (1:200; Jackson Immuno Research). These samples were counterstained with the DNA stain, Topro-3 (Invitrogen, Rockville, MD, U.S.A.). The slides were analysed using confocal laser microscopy (D-Eclipse C1 Nikon, Tokyo, Japan).

Ultrastructural immunohistochemistry

Brain tissues were immersed for 2 h in a fixative containing 2% paraformaldehyde and 0.5% glutaraldehyde in 0.1 M phosphate buffer (pH 7.4). The samples were dehydrated in dimethylformamide and embedded in London Resin Gold (Electron Microscopy Science, Washington, DC, U.S.A.). Ultrathin sections were mounted on uncoated nickel grids and processed for immunocytochemistry (Peruzzo et al., 2000). For immunostaining, rabbit anti-GK antibody was diluted 1:100 in Tris/HCl (pH 7.8) buffer containing 8.4 mM sodium phosphate, 3.5 mM potassium phosphate, 120 mM NaCl and 1% BSA. After extensive washing, the ultrathin sections were incubated for 2 h at 20°C with 10-nm colloidal gold-labelled anti-rabbit IgG (1:20). Uranyl acetate/lead citrate was used as contrast, and samples were analysed using a Hitachi H-700 electron microscope with 125–200 kV accelerating voltage.

In situ hybridization

A PCR product of 510 bp obtained from the hypothalamus was subcloned into pCR-4-Blunt-TOPO (Clontech, Palo Alto, CA, U.S.A.) and was used to generate sense and antisense DIG (digoxigenin)-labelled riboprobes. RNA probes were labelled with DIG-UTP by *in vitro* transcription with SP6 or T7 RNA polymerase by following the manufacturer's procedure (Boehringer–Mannheim). *In situ* hybridization was performed on rat frontal brain sections mounted on poly-L-lysine-coated glass slides (Garcia et al., 2005). The sections were baked at 60°C for 1 h, deparaffinized in xylene, and rehydrated in

graded ethanol. After proteinase K treatment (5 min at 37°C in PBS, 1 μg/ml), the tissue sections were fixed with 4% paraformaldehyde at 4°C for 5 min, washed in cold PBS and then acetylated with 0.1 M triethanolamine/HCl (pH 8.0) and 0.25% acetic anhydride at 20°C for 10 min. After a brief wash, the sections were incubated in pre-hybridization solution at 37°C for 30 min and then 25 μl of a hybridization mixture [50% formamide, 0.6 M NaCl and 10 mM Tris/HCl, pH 7.5, 1 mM EDTA, 1 × Denhardt's solution (0.02% Ficoll 400/0.02% polyvinylpyrrolidone/0.02% BSA), 10% poly(ethylene glycol) 8000, 10 mM DTT (dithiothreitol), 500 μg of yeast tRNA/ml, 50 μg/ml heparin, 500 μg/ml DNA carrier and 1:20 to 1:100 dilutions of riboprobe] were added to each slide. The slides were covered with glass coverslips and placed in a humidified chamber at 42°C overnight. After the removal of the coverslips, the slides were rinsed in 4 × SSC (1 × SSC is 0.15 M NaCl/0.015 M sodium citrate) and washed twice for 30 min at 42°C. The slides were washed at 37°C for 30 min each in 2 × SSC, 1 × SSC and 0.3 × SSC. Visualization of DIG was performed by incubation with a monoclonal antibody coupled with alkaline phosphatase (anti-DIG alkaline phosphatase Fab fragments diluted 1:500; Boehringer–Mannheim) at 20°C for 2 h. Nitro Blue Tetrazolium and BCIP (5-bromo-4-chloroindol-3-yl phosphate; Boehringer–Mannheim) were used as substrates for the alkaline phosphatase. Controls included the use of the sense riboprobe and omission of the probe.

RT–PCR

The brain of each rat was removed and the hypothalamic area was taken out and further dissected until a region close to the ependymal layer was obtained, and total RNA was isolated using TRIzol® (Invitrogen). For RT–PCR, 1 μg of RNA was incubated in a 10 μl reaction volume containing 10 mM Tris/HCl (pH 8.3), 50 mM KCl, 5 mM $MgCl_2$, 20 units of RNase inhibitor, 1 mM dNTPs, 2.5 μM of oligo(dT) primers, and 50 units of MuLV (murine leukaemia virus) reverse transcriptase (New England Biolabs, Ipswich, MA, U.S.A.) for 10 min at 23°C followed by 30 min at 42°C and 5 min at 94°C. Parallel reactions were performed in the absence of reverse transcriptase to control for the presence of contaminant DNA. For amplification, a cDNA aliquot in a volume of 12.5 μl containing 20 mM Tris/HCl (pH 8.4), 50 mM KCl, 1.6 mM $MgCl_2$, 0.4 mM dNTPs, 0.04 unit of Taq DNA polymerase (Gibco-BRL, Carlsbad, CA, U.S.A.) and 0.4 mM primers was incubated at 94°C for 4 min, 94°C for 15–50 s, 55°C for 30–50 s and 72°C for 30–135 s for 35 cycles. PCR products were separated by 1.2–1.5% agarose-gel electrophoresis and visualized by staining with ethidium bromide. The following set of primers was used to analyse the expression of GK: sense 5′-AAAGATGTTGCCCACCTACGTGCG-3′ and antisense 5′-ATCATGCCGACCTCACATTGGC-3′ (expected product of 510 bp). Additionally, the following set of primers was used to analyse the expression of β-actin: sense 5′-GCTGCTCGTCGACAACGGCTC and antisense 5′-CAAACATGATCTGGGTCATCTTCTC-3′ (expected product 353 bp).

Real-time PCR

RNA samples were treated with DNase I before reverse transcription processing to remove genomic DNA contamination. A total of 2 μg of RNA from each sample was reverse transcribed into cDNA using the SuperScript™ III first-strand synthesis system (Invitrogen) according to the manufacturer's suggested protocol. QRT–PCR (quantitative RT–PCR) reactions were prepared with a LightCycler reaction kit in a final volume of 20 μl containing 2 μl of 250 ng of reverse-transcribed total RNA, 500 nM of primers, 4 mM $MgCl_2$ and 2 μl of LightCycler FastStart DNA Master SYBR Green I (Roche Applied Science). PCR reactions were carried out in capillaries in a LightCycler 2.0 instrument (Roche Applied Science Biosystem, Forster, CA, U.S.A.) and were cycled 40 times. The following set of primers was used to analyse the expression of the housekeeping gene, cyclophilin: sense 5′-TGGAGATGAATCTGTAGGAGGAG-3′ and antisense 5′-TACCACATCCATGCCCTCTAGAA-3′ (expected product of 382 bp). The primers used to detect GK mRNA expression were the same as those used for non-quantitative PCR. The thermal cycling conditions consisted of a pre-incubation for 10 min at 95°C, followed by 40 cycles of denaturation for 10 s at 95°C, annealing for 5 s at 55°C and extension for 10 s at 72°C. All experiments were done in triplicate to verify the results. The relative expression of GK mRNA to cyclophilin mRNA was calculated using the $2^{-\Delta\Delta Ct}$ method. The statistical analysis was performed using Prism version 4.0 software (GraphPad Software, San Diego, CA, U.S.A.). GK expression in each group was compared using the Kruskal–Wallis test (nonparametric ANOVA).

Immunoblotting

Total protein extracts were obtained from rat periventricular hypothalamus, liver and pancreas by homogenizing the tissue in buffer A (0.3 mM sucrose, 3 mM DTT, 1 mM EDTA, 100 μg/ml PMSF, 2 μg/ml pepstatin A, 2 μg/ml leucopeptin, and 2 μg/ml aprotinin) and sonicating on ice at 300 W (VCF1, Sonics and Material) three times for 10 s and centrifuging at 4000 ***g*** for 10 min. Proteins were resolved by SDS/PAGE (70 μg per lane) in a 5–15% (w/v) polyacrylamide gel, transferred to PVDF membranes (0.45 μm pore, Amersham Biosciences., Piscataway, NJ, U.S.A.), and probed with rabbit anti-GK or sheep anti-GK antibodies. The reaction was developed using the ECL® Western-blot analysis system (Amersham Biosciences, Pittsburgh, PA, USA).

Nuclear extract preparation

To analyse the subcellular localization of GK *in situ*, hypothalamic nuclear extracts were prepared using the following protocol. Unicellular suspensions were obtained from the dissected tissues by trypsinization followed by disruption in ice-cold PBS with protease inhibitors, DNase I, 3 mM DTT and 1 mM EDTA. Cells were collected after centrifugation at 700 ***g*** for 5 min and resuspended in

ice-cold lysis buffer for 10 min. After centrifugation at 850 *g* for 1 min, the cell pellets were resuspended in hypo-osmotic buffer (10 mM Hepes, 1.5 mM $MgCl_2$ and 10 mM KCl, pH 7.9). The nuclei were isolated by centrifugation at 4600 *g* (Micromax RF centrifugue; IEC) for 1 min, and the nuclear pellets were resuspended in extraction buffer (20 mM Hepes, 1.5 mM $MgCl_2$, 420 mM KCl, 0.2 mM EDTA and 20% glycerol, pH 7.9) and agitated on an orbital shaker at maximum speed in a cold chamber for 45 min followed by centrifugation at 9300 *g* for 5 min. Nuclear extract aliquots were frozen in liquid nitrogen and stored at −80°C. All procedures following the cell disruption were performed on ice or at 4°C. The purity of the nuclear extracts was confirmed by Western-blot analysis using the antibody TFIIB (transcription factor IIB; sc-225, Santa Cruz Biotechnology), a nuclear marker.

RESULTS

GK is expressed in the hypothalamus

The expression of GK in rat hypothalamus was analysed by RT–PCR with primers specific for GK mRNA (Figure 1A, lane 1). The amplified DNA band was approx. 510 bp, which was the expected size for the GK amplification product. The PCR product was sequenced and showed 100% homology with hepatic or pancreatic GK (results not shown). The PCR conditions were optimized using RNA from rat liver and pancreas as positive controls for GK expression (Figure 1A, lanes 2 and 3) and spleen tissue as a negative control (Figure 1A, lane 4) (Iynedjian et al., 1986; Waeber et al., 1994). No amplification product was observed in samples of hypothalamus in the absence of reverse transcriptase (Figure 1A, lane 5). GK expression was also evaluated by Western-blot analysis using protein extracts isolated from rat liver, pancreas and hypothalamus. First, we verified the reactivity of two different anti-GK antibodies (sheep and rabbit) (Figure 1B, lanes 1 and 2). Both antibodies recognized the same band (54 kDa) in liver extracts. Additionally, a similar band was detected in pancreas and hypothalamic protein extracts using rabbit anti-GK (Figure 1B, lanes 3 and 4). Rabbit anti-GK specificity was further analysed by immunohistochemistry in control tissues: liver, pancreas and insulinoma INS-1 cells (see Supplementary Figures S1A–S1G at http://www.asnneuro.org/an/002/an002e035add.htm). Additionally, we demonstrated that rabbit and sheep anti-GK antibodies showed the same GK distribution in liver cells (Supplementary Figures S1H–S1J). Thus sheep anti-GK was used to perform GK and GLUT2 co-localization analyses in brain cells. Cytoplasmic GK expression was confirmed in ventricular ependymal cells (Figures 1D and 1G), which also express GLUT2 localized in the cilia (Figures 1C and 1F).

Morphological characterization of tanycytes and GK mRNA distribution

Prior to analysing GK in hypothalamic tissue, anti-vimentin antibodies were used to define the exact localization of tanycytes in the rat brain (Figure 2). Using confocal microscopy analysis and *Z*-stack projection in the *X*–*Y* and *X*–*Z* planes (Figure 2C), we observed strong immunoreaction for the anti-vimentin antibodies in the periventricular bodies of cells and processes that are in contact with the ventromedial (α) and arcuate nucleus (β) neurons (Figures 2A–2C). Additionally, ultrastructural analysis (Figures 2D–2F) confirmed the classical morphological characteristics of ventricular β-tanycytes: namely microvilli and bleb projections in the apical region of cells (Figures 2D and 2E) and long processes that are in direct contact with hypothalamic neurons (Figure 2F, arrows). This structural association is essential for glia–neuron metabolic interaction. Scanning microscopy analysis revealed the transition between ciliated ependymal cells and tanycytes (Figures 2G–2I) with microvilli (α-tanycytes) or blebs (β-tanycytes) in the apical membrane.

We analysed GK mRNA expression by *in situ* hybridization using DIG-labelled cRNA probes specific for GK (Figures 3A–3F). A positive hybridization signal concentrated in the region facing the third ventricle was detected in both α and β hypothalamic tanycytes (Figures 3C–3E). Although neurons showed a very low hybridization signal, the signal was not concentrated in the arcuate or the ventromedial nucleus (Figures 3D and 3F). The reaction detected in tanycytes was completely abolished when the sense probe was used (Figure 3B).

Optic and ultrastructural analyses of nuclear and cytosolic GK distributions in hypothalamic tanycytes

To establish the precise localization of GK in the hypothalamus of adult rats, immunocytochemical detection and confocal microscopy analyses were employed (Figure 4). Intense anti-GK immunoreactivity was detected in periventricular glial cells co-expressing vimentin (Figures 4A and 4B). A weaker reaction was observed in some hypothalamic neurons (Figure 4A); however, astrocytes and endothelial cells were negative (Figures 4E–4L). Quantitative immunoreaction analysis revealed that GK was preferentially expressed in periventricular glial cells or tanycytes (Figure 4D). Additionally, we demonstrated that GK was preferentially localized in tanycyte nuclei (Figures 4M–4O). A lower immunoreaction was also detected in the tanycytes cytosol (Figure 4O and the inset). In order to confirm GK nuclear detection, Western-blot analysis was performed using nuclear protein extracts isolated from the periventricular hypothalamus. The purity of the nuclear extracts was confirmed using anti-TFIIb (Figure 4P) and GK localization was confirmed by using rabbit anti-GK.

Ultrastructural immunohistochemistry showed GK nuclear localization in tanycytes (Figures 5C and 5D). GK was

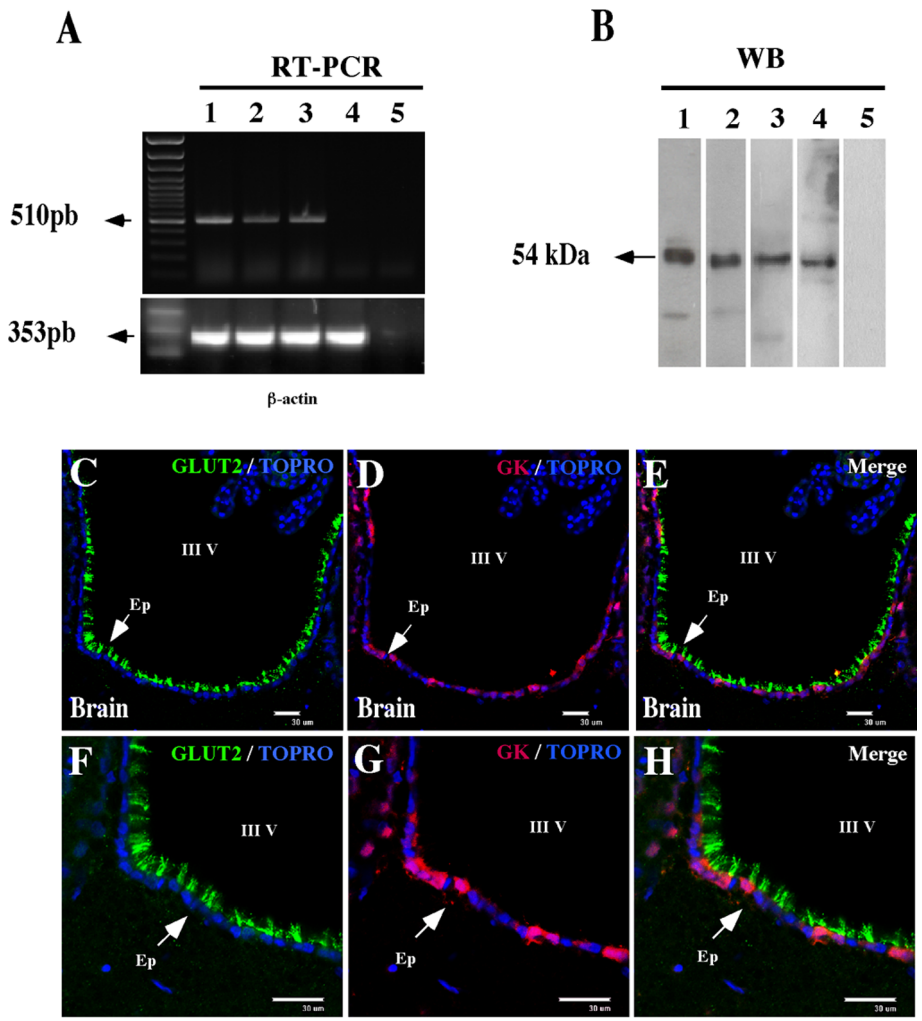

Figure 1 **RT–PCR, Western-blot and immunohistochemical analyses of GK expression**
(**A**) RT–PCR for GK mRNA using mRNAs isolated from pancreas, liver and hypothalamus. Left-hand lane, DNA 100 bp standard; lane 1, amplified sequence of 510 bp using mRNA from rat adult hypothalamus; lane 2, RT–PCR product obtained using mRNA isolated from rat liver; lane 3, RT–PCR product obtained using mRNA isolated from rat pancreas; lane 4, RT–PCR product obtained using mRNA isolated from rat spleen (negative control); lane 5, RT(−) of hypothalamus. (**B**) Western-blot analysis using two different antibodies for human GK. Lane 1, sheep anti-GK and rat liver extract; lanes 2–4, rabbit anti-GK and rat liver (2), pancreas (3) and hypothalamus (4) extracts; lane 5, control using hypothalamic extract. (**C–G**) Frontal sections of rat brain immunostained with sheep anti-GK and rabbit anti-GLUT2 antibodies followed by secondary antibodies labelled with Cy3 (red) or Cy2 (green). Topro-3 was used for nuclear staining. GK immunoreactivity is detected in the cytosol of ependymal cells and GLUT2 is detected in the ciliar membranes. III V, third ventricle; Ep, ependymal cells. Scale bars in (**C–H**), 30 μm.

detected in the apical region of the tanycytes (Figures 5A and 5B); however, the blebs and microvilli were almost negative. To confirm the apical localization of GK as well as GLUT2 and GK co-distribution in tanycytes, we used confocal microscopy analysis and *Z*-stack projection to increase the positive GK signal (Figure 6). A diffuse GLUT2 distribution was detected in tanycytes (Figures 6A and 6D); however, most of the cells showed stronger immunoreactivity in the apical region (Figure 6D). After *Z*-stack projection analysis, GK immunoreaction was clearly detected in the nuclei as well as the apical region of tanycytes (Figures 6B and 6E). GK and GLUT2 co-localization was mainly detected in the apical region of the cells but not in the nucleus (Figures 6C and 6F).

Additionally, immunofluorescent staining and confocal microscopy were used to demonstrate broad GK distribution in different hypothalamic regions (Supplementary Figure S2 at http://www.asnneuro.org/an/002/an002e035add.htm).

GK is induced during post-natal development in hypothalamic tanycytes

GK levels during post-natal development were assessed by immunohistochemistry and RT–PCR analyses (Figure 7). The intensity of the GK immunoreactivity markedly increased during the second week of post-natal development; on day 10 of the post-natal period, positive GK immunoreaction was

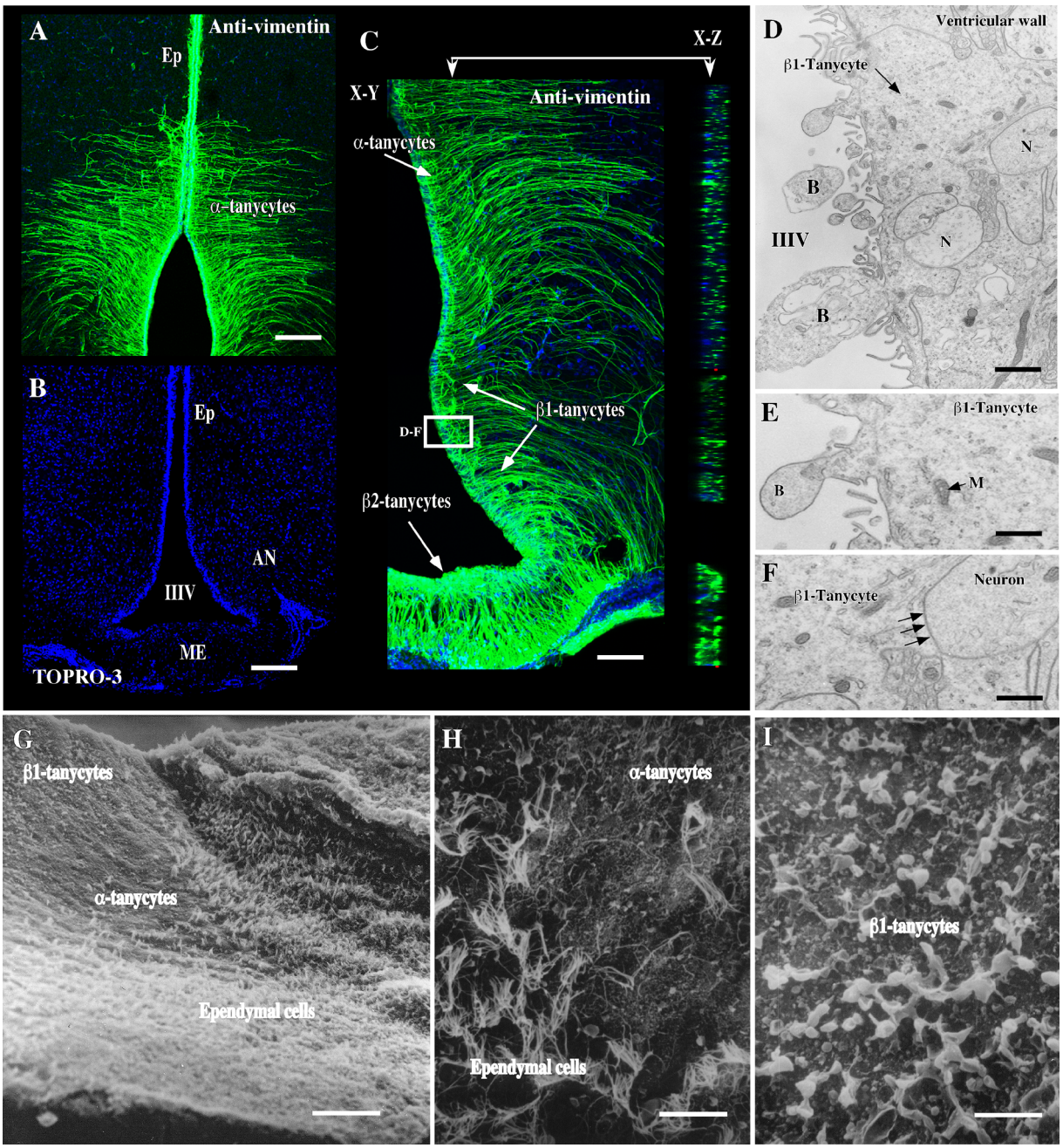

Figure 2 **Immunohistochemical and ultrastructural analysis of the hypothalamic tanycytes**
(**A–C**) Frontal hypothalamic sections immunostained with anti-vimentin antibody and using a secondary antibody labelled with Cy2. Topro-3 was used for nuclear staining. *Z*-stack sections were obtained using confocal analysis and are shown in *X–Y* and *X–Z* projection (**C**). (**D–F**) Transmission electron microscopy of the ventricular wall. The area analysed is framed in (**C**). The association between tanycytes and neuron is shown (N). (**E**) The β1-tanycytes present blebs (B) in the apical region of the cells. (**F**) Contact region between tanycytes and neurons (arrows). (**G–I**) Scanning electron microscopy of the ventricular wall associated with the hypothalamic basal area. (**H**) Transition between ependymal cells and α-tanycytes. (**I**) Scanning microscopy of blebs present in the apical region of β-tanycytes. III V, third ventricle; Ep, ependymal cells; ME, median eminence; M, mitochondrion. Scale bar in (**A–C**), 150 μm; scale bars in (**D–F**), 1 μm; scale bar and in (**G**), 100 μm; scale bars in (**H** and **I**), 25 μm.

detected within tanycytes, suggesting early GK expression and biosynthesis (Figures 7A–7D, arrows). This immunoreaction was mainly detected in vimentin-positive cells, confirming GK expression in tanycytes (Figures 7D, 7H and 7L). On days 15 and 20, immunoreaction was detected in tanycyte cytoplasm, but not in nuclei (Figures 7E–7L). Finally, GK levels during post-natal development was confirmed by RT–PCR (Figure 7M). Furthermore, GK mRNA QRT–PCR analysis was

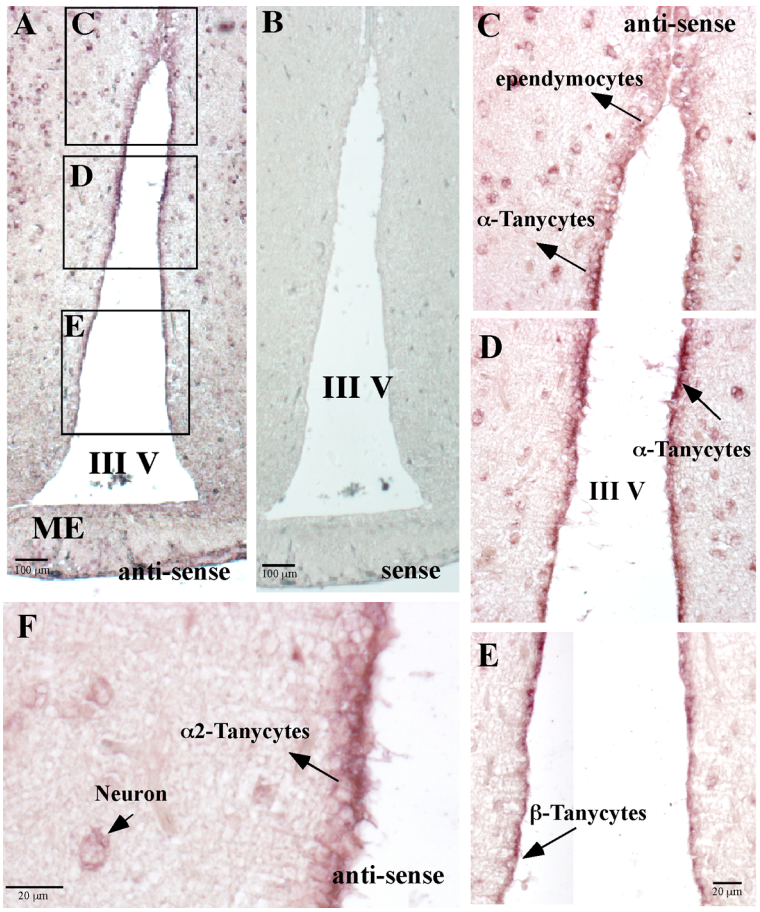

Figure 3 **Glial GK mRNA detection by *in situ* hybridization**
Frontal section of rat hypothalamus probed with a GK antisense riboprobe. (**A**) A high hybridization signal was observed in glial cells of the periventricular area. (**B**) The sense riboprobe for GK was used as a control. (**C–F**) The α- and β1-tanycytes present positive hybridization with the antisense GK riboprobe. In α- and β1-tanycytes, the positive reaction is observed in the proximal area of the cells. Also some neurons show a positive reaction for the GK riboprobe (**F**). III V, third ventricle; ME, median eminence. Scale bars in (**A** and **B**), 100 μm; in (**C–F**), 20 μm.

carried out (Figure 7N). Whereas GK was initially present in the hypothalamus at equivalent levels for the first 5 days, additional brain post-natal development was accompanied by a marked increase in the amount of GK. Specifically, on days 10 and 15, the amount of GK mRNA was approx. 3- and 8-fold greater than that on day 1 respectively.

DISCUSSION

Different hypothalamic areas as well as others regions within the brain, specifically the area postrema, medulla oblongata and tractus solitarius nucleus, are believed to have glucose-sensing mechanisms that modulate feeding behaviour (Frizzell et al., 1993; Leloup et al., 1998; Roncero et al., 2004; Schwartz et al., 2000; Wan et al., 1998). Similar to β-cells of the pancreas, previous studies indicate that GK and GLUT2 expression in these brain areas is essential to detect changes in blood glucose concentration (Bady et al., 2006; Leloup et al., 1998; Lynch et al., 2000; Maekawa et al., 2000; Marty et al., 2005; Yang et al., 2007).

In situ hybridization analysis has revealed GK and GLUT2 expression in a region of the hypothalamus containing neurons and ependymal cells (Lynch et al., 2000; Navarro et al., 1996; Yang et al., 1999). However, the low resolution capacity of the radioautographic detection of the GK probe prevented identification of the cell types expressing GK and GLUT2. The *in situ* non-isotopic hybridization carried out in the present study clearly identifies α- and β-tanycytes as the main hypothalamic cells positive for GK expression; however, a reduced hybridization signal in neuronal soma (arcuate nucleus) was also detected. Additionally, we performed a detailed immunohistochemical analysis of GK expression in rat hypothalamic tanycytes using two different antibodies that showed the same pattern of immunostaining. The tanycyte subpopulation expressing GK and GLUT2 was also identified. As

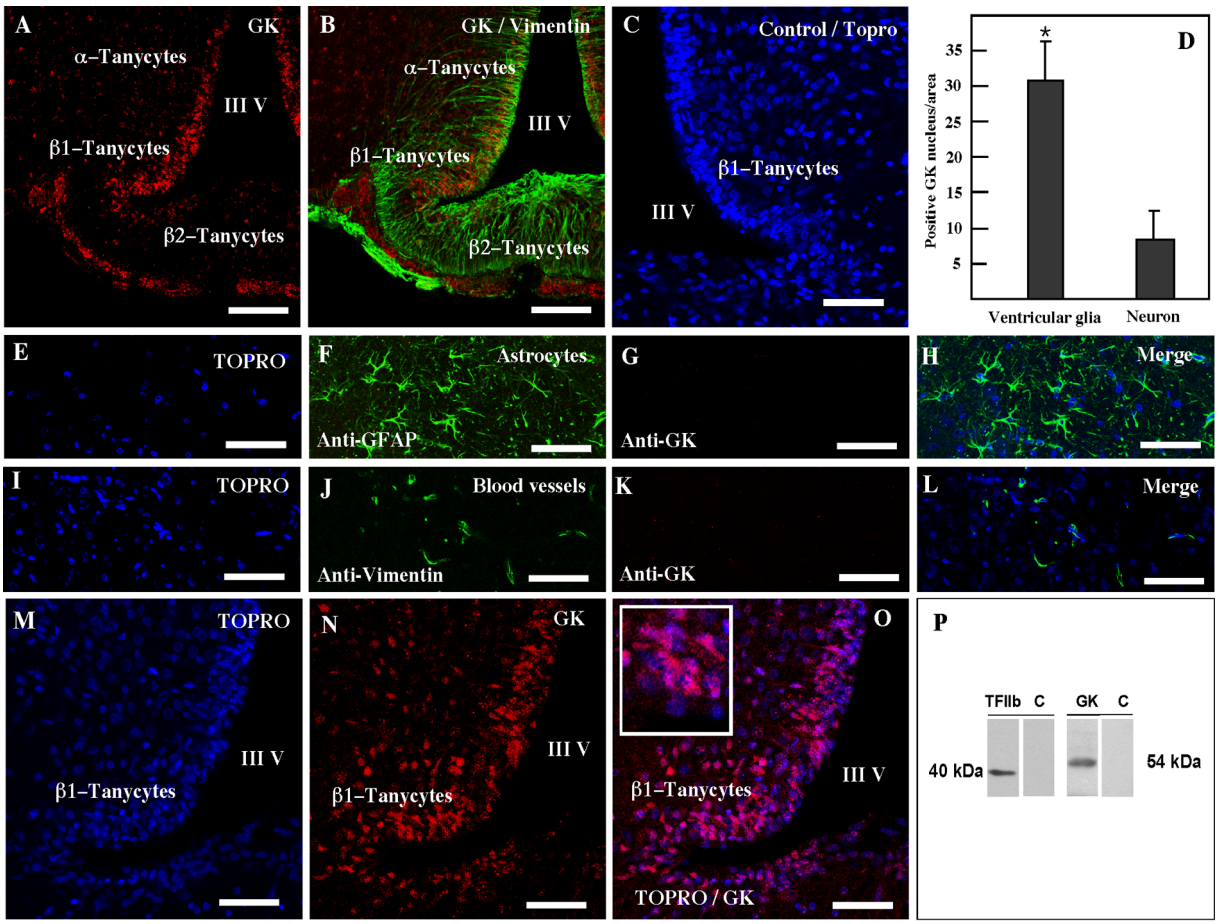

Figure 4 **GK and vimentin are co-localized in the ventricular tanycytes**

(**A** and **B**) Frontal hypothalamic sections immunostained with anti-vimentin and anti-GK antibodies and using a secondary antibody labelled with Cy3 (red) and Cy2 (green). (**C**) A frontal hypothalamic section used as a control. (**D**) Quantitative analysis of GK-positive nuclei in tanycytes and neurons. Statistical analysis was performed using the Student's *t* test with Welch correction; *P* values$<$0.05 were considered significant. Results represent the average GK-positive nuclei in a total of 16 areas within the ventricular and arcuate nuclei. (**E–H**) Brain sections co-immunostained with anti-GFAP (astrocytes marker) and sheep anti-GK. (**I–L**) Brain sections co-immunostained with anti-vimentin (blood vessels marker) and rabbit anti-GK. (**M–O**) Frontal hypothalamic sections immunostained with rabbit anti-GK using a secondary antibody labelled with Cy3 (red) and Topro-3 (blue) for nuclear staining. GK is mainly detected in the nucleus of tanycytes (the inset and merged image in O). (**P**) Western-blot study using nuclear protein extracts isolated from the periventricular hypothalamus and analysed with rabbit anti-GK and anti-TFIIb antibodies. III V, third ventricle. Scale bars in (**A** and **B**), 100 μm; scale bars in (**C** and **M–O**), 50 μm; scale bars in (**E–L**), 150 μm.

observed in liver cells, optic and ultrastructural microscopic analyses showed preferential GK immunoreaction in the nucleus of α- and β-tanycytes. In pancreas and insulinoma ISN-1 cells, GK was not detected in the nucleus; positive immunostaining was observed only in the cytoplasm, confirming the specificity of GK antibodies. Other hypothalamic cells, such as astrocytes and endothelial cells, were consistently negative for GK immunoreactivity; however, some neurons in the arcuate nuclei were positive for GK. To increase GK detection, we used 40 μm slides for confocal laser microscopy and *Z*-stack projection, confirming nuclear GK distribution as well as its localization in the apical cytoplasmic region of tanycytes and ependymal cells of the third ventricle.

Our results are consistent with initial immunocytochemical analyses of GK expression, which revealed that this protein has a wide distribution in the ependymal cells of ventricular cavities (Maekawa et al., 2000). GK and GLUT2 expression has been localized in ciliated ependymal cells of the cerebral ventricles, specifically in the cell membrane of the cilia (Maekawa et al., 2000), which is similar to our results. However, no immunoreaction was observed in the low wall of the third ventricle, the tanycytes region. It is possible that the difference could be attributed to the use of different antibodies. The antibodies used in the present study recognize pancreatic and hepatic GK; however, the antibody used by Maekawa et al. (2000) reacted specifically with the pancreatic isoform. Nuclear GK localization in tanycytes strongly suggests GKRP co-expression in these cells. Alvarez et al. (2002) demonstrated GKRP expression in the hypothalamus; GKRP mRNA was detected in the periventricular nucleus. However, a detailed

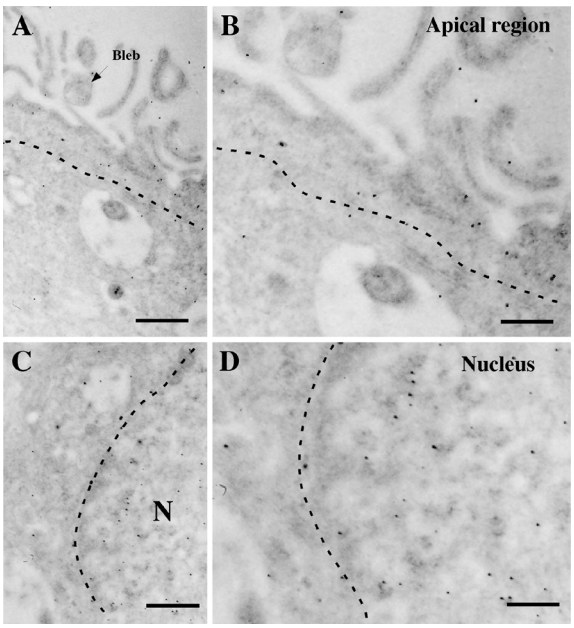

Figure 5 Ultrastructural immunocytochemistry of hypothalamic ventricular wall

Frontal section through the rat medial basal hypothalamus. Immunohistochemical analysis using rabbit anti-GK antibody and anti-IgG labelled with 10-nm gold particles. (**A**, **B**) Apical region of β1-tanycytes. The immunoreaction is mainly observed in the apical region of the cells, depicted over the segment line. (**C**, **D**) Nuclear region of β1-tanycytes. Stronger immunostaining was detected that is associated with the chromatin. III V, third ventricle; N, nucleus. Scale bars in (**A**, **C**), 1 μm; scale bars in (**B**, **D**), 0.5 μm.

analysis of the hybridization signal strongly suggests a positive reaction in glial periventricular cells. Therefore subcellular translocation of GK may regulate its activity in tanycytes in accordance with the metabolic needs of the cell.

Using rat hypothalamic slices, Sanz et al. (2007) reported GK expression and functional activity in ventromedial hypothalamus and lateral hypothalamus areas. They also analysed the effects of glucose and insulin on GK activity in rat hypothalamus and demonstrated that GK activity was modified by these molecules. Additionally, they postulated that altered GK activity may be associated with specific cells in defined brain areas. Because tanycytes express GK and are in contact with ventromedial and lateral hypothalamic neurons, tanycytes may also modify GK activity.

In the periventricular hypothalamus, the interaction between hypothalamic neurons and glial periventricular cells may be necessary for glucose sensing. Our previous study revealed that astrocytes were absent from areas containing α- and β1-tanycytes. In the hypothalamus, tanycytes are the primary glial cell in contact with the CSF, blood and neurons (Garcia et al., 2001). Therefore the expression of GLUT2 and GK in hypothalamic tanycytes may have important physiological consequences. An elevated K_m for glucose transport and the presence of GK imply that tanycytes increase their glucose uptake rate in direct proportion to extracellular changes in glucose concentration. This property of GLUT2 and GK determines their participation in the glucose-sensing mechanism of pancreatic β-cells (Guillam et al., 1997, 2000; Iynedjian, 2009; Schuit et al., 2001; Yang et al., 1999). Therefore GLUT2 and GK may play a similar role in hypothalamic tanycytes. Sanders et al. (2004) injected alloxan, a GK inhibitor and toxin, into the third ventricle, demonstrating that treated rats exhibited impaired feeding behaviour and blood glucose concentration. These impaired responses were associated with the destruction of third ventricle tanycytes, neuronal swelling and decreased arcuate nucleus neuropeptide Y mRNA. However, 2 weeks after

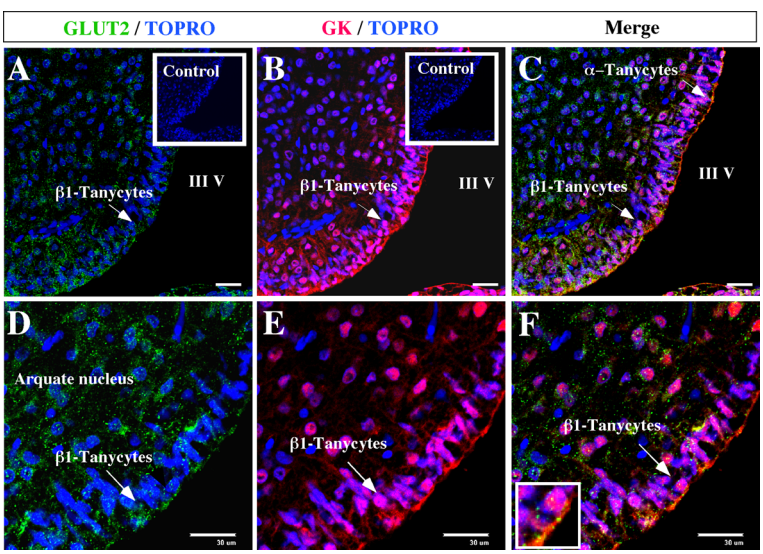

Figure 6 **GK and GLUT2 expressions in the ventricular tanycytes**

(**A–F**) Frontal hypothalamic sections immunostained with anti-GLUT2 and sheep anti-GK antibodies and using a secondary antibody labelled with Cy2 (green) or Cy3 (red). Topro-3 (blue) was used for nuclear staining. Confocal analysis and *Z*-stack projection confirmed GK and GLUT2 co-localization in the apical region of the tanycytes. Nuclear staining was also detected. Insets: negative controls. III V, third ventricle. Scale bars in (**A–C**), 50 μm; scale bars in (**D–F**), 30 μm.

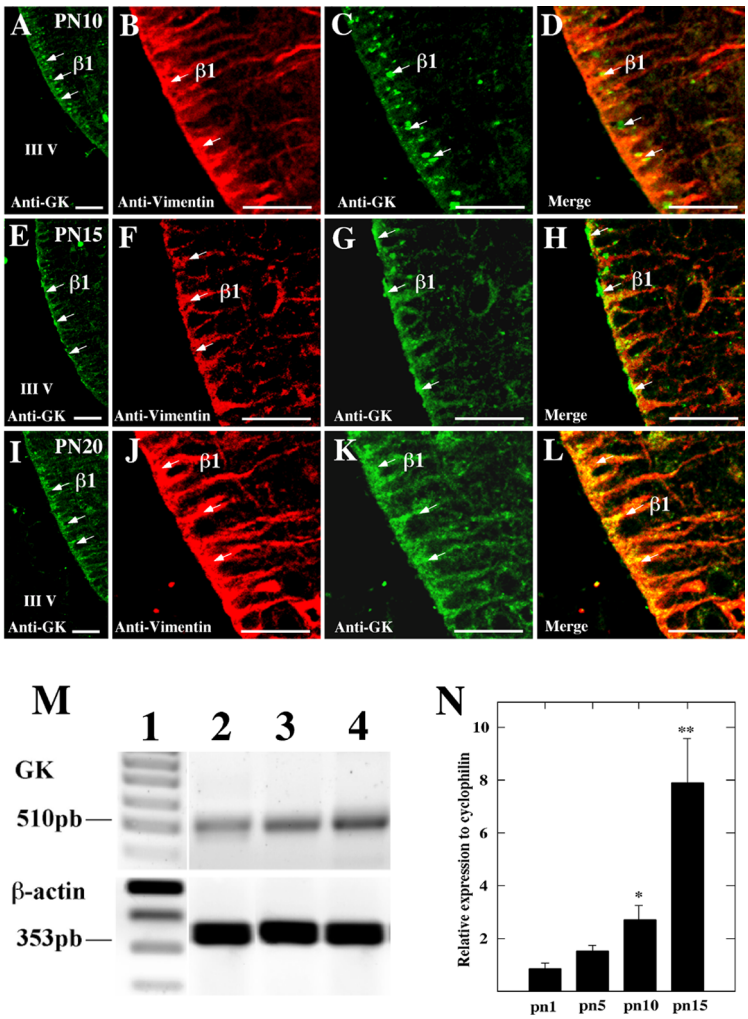

Figure 7 **GK levels during post-natal tanycyte development**

Frontal hypothalamic sections through the rostral hypothalamic region immunostained with rabbit anti-GK (green) or and anti-vimentin (red). (**A–D**) Post-natal 10-day-old (PN10). (**E–H**) Post-natal 15-day-old (PN15). (**I–L**) Post-natal 20-day-old (PN20). (**M**) RT–PCR analysis. Lane 1, 100 bp standard; lane 2, RT–PCR product obtained using mRNA isolated from 1-day-old rat hypothalamus; lane 3, mRNA isolated from 5-day-old rat hypothalamus; lane 4, mRNA isolated from 15-day-old rat hypothalamus. (**N**) QRT–PCR analysis of the mRNA GK levels in samples isolated from 1-day-old rat hypothalamus (pn1), 5-day-old rat hypothalamus (pn5), 10-day-old rat hypothalamus (pn10) and 15-day-old rat hypothalamus (pn15). *P values <0.05; **P values <0.01. Results are the ratio of GK mRNA to cyclophilin mRNA and represent the means $\pm$ S.D. for three independent experiments. III V, third ventricle. Scale bars in (**A–L**), 100 μm.

alloxan injection, third ventricle tanycyte destruction was reversed; this was accompanied by restoration of feeding and hyperglycaemic responses to both systemic and hindbrain glucoprivation. Interestingly, in genetic complementation experiments in which a GLUT2 cDNA was expressed in Ripglut1;glut2$^{-/-}$ mice under the control of the GFAP (glial-specific) or the synapsin (neuron-specific) promoters, counter-regulation was restored only when GLUT2 was expressed in glial cells (Marty et al., 2005). According to a previously published hypothesis, the glia cell may take up glucose through GLUT2, catabolize it to lactate and transfer lactate to neurons via monocarboxylate transporters for production of ATP through further degradation by the tricarboxylic acid cycle (Ainscow et al., 2002).

GK levels were strongly up-regulated during the second week of post-natal development. This suggests that GK functional activity is increased when the blood–brain barrier reaches the mature level with the weaning (Vorbrodt et al., 2001). In the second week, GK was broadly distributed in the cytoplasm of the tanycytes but not in the nucleus. A similar subcellular distribution has been observed in liver cells. Before day 11 post-partum, only some hepatocytes were immunostained, and a positive reaction was found in the cytoplasm but not in the nucleus of the cells (Toyoda et al., 1995b). These results suggest that nuclear compartmentalization may be associated with post-natal GKRP co-expression, a condition that has not been analysed in hypothalamic tanycytes or liver cells.

ACKNOWLEDGEMENTS

We thank Dr Marjet Heitzer (University of Pittsburgh, Pittsburgh, PA, U.S.A.) for a critical review of this paper prior to acceptance, and Ms Ximena Koch for technical assistance.

FUNDING

This work was supported by the CONICYT (Comisión Nacional de Investigación Científica y Tecnológica)–World Bank [grant number ACT02] and University of Concepcion [grant number DIUC 205.031.101-1.0].

REFERENCES

Ainscow EK, Mirshamsi S, Tang T, Ashford ML, Rutter GA (2002) Dynamic imaging of free cytosolic ATP concentration during fuel sensing by rat hypothalamic neurones: evidence for ATP-independent control of ATP-sensitive K(+) channels. J Physiol 544:429–445.

Akmayev IG, Popov AP (1977) Morphological aspects of the hypothalamic–hypophyseal system. VII. The tanycytes: their relation to the hypophyseal adrenocorticotrophic function. An ultrastructural study. Cell Tissue Res 180:263–282.

Alvarez E, Roncero I, Chowen JA, Vazquez P, Blazquez E (2002) Evidence that glucokinase regulatory protein is expressed and interacts with glucokinase in rat brain. J Neurochem 80:45–53.

Bady I, Marty N, Dallaporta M, Emery M, Gyger J, Tarussio D, Foretz M, Thorens B (2006) Evidence from glut2-null mice that glucose is a critical physiological regulator of feeding. Diabetes 55:988–995.

Bali D, Svetlanov A, Lee HW, Fusco-DeMane D, Leiser M, Li B, Barzilai N, Surana M, Hou H, Fleischer N, DePinho R, Rossetti L, Efrat S (1995) Animal model for maturity-onset diabetes of the young generated by disruption of the mouse glucokinase gene. J Biol Chem 270:21464–21467.

Frizzell RT, Jones EM, Davis SN, Biggers DW, Myers SR, Connolly CC, Neal DW, Jaspan JB, Cherrington AD (1993) Counterregulation during hypoglycemia is directed by widespread brain regions. Diabetes 42:1253–1261.

Garcia M, Salazar K, Millan C, Rodriguez F, Montecinos H, Caprile T, Silva C, Cortes C, Reinicke K, Vera JC, Aguayo LG, Olate J, Molina B, Nualart F (2005) Sodium vitamin C cotransporter SVCT2 is expressed in hypothalamic glial cells. Glia 50:32–47.

Garcia MA, Carrasco M, Godoy A, Reinicke K, Montecinos VP, Aguayo LG, Tapia JC, Vera JC, Nualart F (2001) Elevated expression of glucose transporter-1 in hypothalamic ependymal cells not involved in the formation of the brain-cerebrospinal fluid barrier. J Cell Biochem 80:491–503.

Garcia MA, Millan C, Balmaceda-Aguilera C, Castro T, Pastor P, Montecinos H, Reinicke K, Zuniga F, Vera JC, Onate SA, Nualart F (2003) Hypothalamic ependymal-glial cells express the glucose transporter GLUT2, a protein involved in glucose sensing. J Neurochem 86:709–724.

Guillam MT, Dupraz P, Thorens B (2000) Glucose uptake, utilization, and signaling in GLUT2-null islets. Diabetes 49:1485–1491.

Guillam MT, Hummler E, Schaerer E, Yeh JI, Birnbaum MJ, Beermann F, Schmidt A, Deriaz N, Thorens B (1997) Early diabetes and abnormal postnatal pancreatic islet development in mice lacking Glut-2. Nat Genet 17:327–330.

Iynedjian PB (2009) Molecular physiology of mammalian glucokinase. Cell Mol Life Sci 66:27–42.

Iynedjian PB, Mobius G, Seitz HJ, Wollheim CB, Renold AE (1986) Tissue-specific expression of glucokinase: identification of the gene product in liver and pancreatic islets. Proc Natl Acad Sci USA 83:1998–2001.

Kang L, Dunn-Meynell AA, Routh VH, Gaspers LD, Nagata Y, Nishimura T, Eiki J, Zhang BB, Levin BE (2006) Glucokinase is a critical regulator of ventromedial hypothalamic neuronal glucosensing. Diabetes 55:412–420.

Kang L, Routh VH, Kuzhikandathil EV, Gaspers LD, Levin BE (2004) Physiological and molecular characteristics of rat hypothalamic ventromedial nucleus glucosensing neurons. Diabetes 53:549–559.

Leloup C, Orosco M, Serradas P, Nicolaidis S, Penicaud L (1998) Specific inhibition of GLUT2 in arcuate nucleus by antisense oligonucleotides suppresses nervous control of insulin secretion. Mol Brain Res 57:275–280.

Lynch RM, Tompkins LS, Brooks HL, Dunn-Meynell AA, Levin BE (2000) Localization of glucokinase gene expression in the rat brain. Diabetes 49:693–700.

Maekawa F, Toyoda Y, Torii N, Miwa I, Thompson RC, Foster DL, Tsukahara S, Tsukamura H, Maeda K (2000) Localization of glucokinase-like immunoreactivity in the rat lower brain stem: for possible location of brain glucose-sensing mechanisms. Endocrinology 141:375–384.

Marty N, Dallaporta M, Foretz M, Emery M, Tarussio D, Bady I, Binnert C, Beermann F, Thorens B (2005) Regulation of glucagon secretion by glucose transporter type 2 (glut2) and astrocyte-dependent glucose sensors. J Clin Invest 115:3545–3553.

Navarro M, Rodriquez de Fonseca F, Alvarez E, Chowen JA, Zueco JA, Gomez R, Eng J, Blazquez E (1996) Colocalization of glucagon-like peptide-1 (GLP-1) receptors, glucose transporter GLUT-2, and glucokinase mRNAs in rat hypothalamic cells: evidence for a role of GLP-1 receptor agonists as an inhibitory signal for food and water intake. J Neurochem 67:1982–1991.

Peruzzo B, Pastor FE, Blazquez JL, Schobitz K, Pelaez B, Amat P, Rodriguez EM (2000) A second look at the barriers of the medial basal hypothalamus. Exp Brain Res 132:10–26.

Roncero I, Alvarez E, Chowen JA, Sanz C, Rabano A, Vazquez P, Blazquez E (2004) Expression of glucose transporter isoform GLUT-2 and glucokinase genes in human brain. J Neurochem 88:1203–1210.

Roncero I, Alvarez E, Vazquez P, Blazquez E (2000) Functional glucokinase isoforms are expressed in rat brain. J Neurochem 74:1848–1857.

Sanders NM, Dunn-Meynell AA, Levin BE (2004) Third ventricular alloxan reversibly impairs glucose counterregulatory responses. Diabetes 53:1230–1236.

Sanz C, Roncero I, Vazquez P, Navas MA, Blazquez E (2007) Effects of glucose and insulin on glucokinase activity in rat hypothalamus. J Endocrinol 193:259–267.

Schuit FC, Huypens P, Heimberg H, Pipeleers DG (2001) Glucose sensing in pancreatic beta-cells: a model for the study of other glucose-regulated cells in gut, pancreas, and hypothalamus. Diabetes 50:1–11.

Schwartz MW, Woods SC, Porte Jr D, Seeley RJ, Baskin DG (2000) Central nervous system control of food intake. Nature 404:661–671.

Terauchi Y, Sakura H, Yasuda K, Iwamoto K, Takahashi N, Ito K, Kasai H, Suzuki H, Ueda O, Kamada N et al. (1995) Pancreatic beta-cell-specific targeted disruption of glucokinase gene. Diabetes mellitus due to defective insulin secretion to glucose. J Biol Chem 270:30253–30256.

Toyoda Y, Miwa I, Kamiya M, Ogiso S, Nonogaki T, Aoki S, Okuda J (1995a) Tissue and subcellular distribution of glucokinase in rat liver and their changes during fasting-refeeding. Histochem Cell Biol 103:31–38.

Toyoda Y, Miwa I, Kamiya M, Ogiso S, Okuda J, Nonogaki T (1995b) Changes in subcellular and zonal distribution of glucokinase in rat liver during postnatal development. FEBS Lett 359:81–84.

Vandercammen A, Van Schaftingen E (1990) The mechanism by which rat liver glucokinase is inhibited by the regulatory protein. Eur J Biochem 191:483–489.

Vandercammen A, Van Schaftingen E (1991) Competitive inhibition of liver glucokinase by its regulatory protein. Eur J Biochem 200:545–551.

Vorbrodt AW, Dobrogowska DH, Tarnawski M (2001) Immunogold study of interendothelial junction-associated and glucose transporter proteins during postnatal maturation of the mouse blood–brain barrier. J Neurocytol 30:705–716.

Waeber G, Thompson N, Haefliger JA, Nicod P (1994) Characterization of the murine high Km glucose transporter GLUT2 gene and its transcriptional regulation by glucose in a differentiated insulin-secreting cell line. J Biol Chem 269:26912–26919.

Wan HZ, Hulsey MG, Martin RJ (1998) Intracerebroventricular administration of antisense oligodeoxynucleotide against GLUT2 glucose transporter mRNA reduces food intake, body weight change and glucoprivic feeding response in rats. J Nutr 128:287–291.

Yang XJ, Kow LM, Funabashi T, Mobbs CV (1999) Hypothalamic glucose sensor: similarities to and differences from pancreatic beta-cell mechanisms. Diabetes 48:1763–1772.

Yang XJ, Mastaitis J, Mizuno T, Mobbs CV (2007) Glucokinase regulates reproductive function, glucocorticoid secretion, food intake, and hypothalamic gene expression. Endocrinology 148:1928–1932.

Received 15 December 2009/8 April 2010; accepted 13 April 2010

Published as Immediate Publication 30 April 2010, doi 10.1042/AN20090059